ECT2 associated to PRICKLE1 are poor-prognosis markers in triple-negative breast cancer

Luc Camoin, Jean-Paul Borg, Avais M Daulat, Pascal Finetti, Diego R Revinski, Mônica Silveira Wagner, Stéphane Audebert, Daniel Birnbaum, Laurent Kodjabachian, François Bertucci

▶ **To cite this version:**

Luc Camoin, Jean-Paul Borg, Avais M Daulat, Pascal Finetti, Diego R Revinski, et al.. ECT2 associated to PRICKLE1 are poor-prognosis markers in triple-negative breast cancer. British Journal of Cancer, 2019, 120 (9), pp.931-940. 10.1038/s41416-019-0448-z . hal-02145896

HAL Id: hal-02145896
https://hal.science/hal-02145896

Submitted on 3 Jun 2019

HAL is a multi-disciplinary open access archive for the deposit and dissemination of scientific research documents, whether they are published or not. The documents may come from teaching and research institutions in France or abroad, or from public or private research centers.

L'archive ouverte pluridisciplinaire **HAL**, est destinée au dépôt et à la diffusion de documents scientifiques de niveau recherche, publiés ou non, émanant des établissements d'enseignement et de recherche français ou étrangers, des laboratoires publics ou privés.

ECT2 associated to PRICKLE1 are poor-prognosis markers in triple-negative breast cancer

Avais M. Daulat[1,*], Pascal Finetti[2], Diego Revinski[1,4], Mônica Silveira Wagner[1], Luc Camoin[3], Stéphane Audebert[3], Daniel Birnbaum[2], Laurent Kodjabachian[4], Jean-Paul Borg[1,3,#,*], and François Bertucci[2,#]

[1]Centre de Recherche en Cancérologie de Marseille, Aix Marseille Univ UM105, Inst Paoli Calmettes, UMR7258 CNRS, U1068 INSERM, «Cell Polarity, Cell signalling and Cancer - Equipe labellisée Ligue Contre le Cancer », Marseille, France

[2]Centre de Recherche en Cancérologie de Marseille, Aix Marseille Univ UM105, Inst Paoli Calmettes, UMR7258 CNRS, U1068 INSERM, «Predictive Oncology team », Marseille, France

[3]Aix Marseille University, CNRS, INSERM, Institut Paoli-Calmettes, CRCM, Marseille Protéomique, Marseille, France

[4] Aix Marseille Univ, CNRS, IBDM, Marseille, France

* To whom correspondence should be addressed: avais.daulat@inserm.fr/jean-paul.borg@inserm.fr/ Phone 33-4-8697-7201, Fax 33-4-8697-7499

Co-lead authors

Keywords: PRICKLE1, ECT2, signaling, therapeutic targets, Triple Negative Breast Cancer

Conflict of interest statement: The authors declare no potential conflicts of interest.

Abstract

Triple negative breast cancer (TNBC) is the most aggressive breast cancer subtype and the lack of specific signature makes difficult the development of targeted therapeutic strategy. We previously found that PRICKLE1, an evolutionary conserved protein acting as a regulator of vertebrate development, is upregulated in TNBC. Proteomic approaches allowed us to decipher the protein complex associated to PRICKLE1 in TNBC. Within that complex, we identified a large subset of proteins involved in the regulation of Rho-GTPase family members. We build a metagene with regulators of small G-protein activity and we found that this metagene is overexpressed in TNBC and is a poor prognosis marker. We analyzed the combination of the metagene expression and *PRICKLE1* expression and identified that combined expression of *ECT2* and *PRICKLE1* provides a worst prognosis than *PRICKLE1* expression alone in TNBC. ECT2 is a GEF for Rac1 and we showed that PRICKLE1 regulate the enzymatic activity of ECT2. Finally, we also observed that Ect2 and Prickle1 are functionally connected during evolution since both act synergistically to coordinate cellular movement during vertebrate gastrulation. Our results demonstrate the pivotal role of PRICKLE1 in TNBC and build the path for development of targeted therapeutic strategies to heal TNBC patients.

Introduction

Triple-negative breast cancer (TNBC) is the most aggressive molecular subtype of breast cancer(Tong et al 2018). In contrast with mammary cancers of other subtypes (HR+/HER2- and HER2+), TNBCs do not express hormone receptors and HER2 oncogene and thus are not candidate to hormone therapy and anti-HER2 therapy (Tong et al 2018). Chemotherapy is the only systemic therapy currently approved for this subtype. However, TNBC is highly invasive with strong metastatic propensity (Tong et al 2018). We recently identified *PRICKLE1* as poor-prognosis marker in breast cancer(Daulat et al 2016). PRICKLE1 is a member of a conserved group of proteins involved in planar cell polarity (PCP) pathway(Butler and Wallingford 2017). This pathway is well characterized in epithelial tissue morphogenesis during embryonic development of invertebrates and vertebrates. The organization of PCP relies on the spatial distribution of proteins at the plasma membrane such as Wnts, Frizzled, Vang Gogh, Flamingo, Dishevelled, Diego, and Prickle. In vertebrates, homologous genes are involved in the regulation of convergent-extension during the early stages of gastrulation which leads to the organization of cells to organize the head-to-tail axis(Butler and Wallingford 2017, Sokol 2015). Prickle1 plays a pivotal role to regulate PCP in Drosophila(Gubb and Garcia-Bellido 1982), as well as convergent-extension in Zebrafish(Veeman et al 2003) and Xenopus(Takeuchi et al 2003). PRICKLE1 is an evolutionary conserved cytoplasmic protein and contains from the amino-terminal end a PET followed by three LIM domains and a C-terminal farnesylation site(Jenny et al 2003). Recently, we and others have demonstrated the prominent role of PRICKLE1 during cancer progression(Daulat et al 2016, Lim et al 2016, Luga et al 2012, Zhang et al 2016). PRICKLE1 is a prometastatic molecule and regulates oriented cell migration in various cell lines including the MDA-MB-231 prototypal TNBC cell line(Daulat et al 2016, Zhang et al 2016). At the molecular level, PRICKLE1 regulates subcellular localization of its associated proteins

such as VANGL2(Daulat et al 2012, Jenny et al 2003), RICTOR(Daulat et al 2016), ARHGAP22/24(Zhang et al 2016), and LL5β(Lim et al 2016) in order to coordinate oriented cellular migration.

Here, we identified the proteome associated to PRICKLE1 in MDA-MB-231 cells. Among the proteins associated to PRICKLE1, our attention was attracted by a large subset of small G-protein regulators. Since regulation of cancer migration depends of the activation of small G-proteins such as Rac, Rho, and Cdc42, we further explored the role of this subset of small G-protein regulators using transcriptomic analysis from publically available data set obtained from patients with breast cancer. We gathered all the identified small G-protein regulators in a metagene to allow an in-depth analysis and showed that *PRICKLE1* was not only overexpressed in TNBC, but its associated proteins were also up-regulated in TNBC and were poor-prognosis markers. To further explore the protein complex associated to PRICKLE1, we focused our attention on the Rho-Guanylyl Exchange Factor (GEF) called Epithelial cell transforming sequence 2 (ECT2). In non-transformed cells, ECT2 regulates cytokinesis by regulating Rac1 activity(Huff et al 2013, Justilien and Fields 2009, Justilien et al 2011, Justilien et al 2017). *ECT2* is frequently up-regulated in various cancers such as ovarian(Huff et al 2013), lung(Zhou et al 2017) and breast cancer(Wang et al 2018). Knockdown of ECT2 inhibits Rac1 activity and block transformed growth, invasion and tumorigenicity(Justilien and Fields 2009, Justilien et al 2011). Here we showed that PRICKLE1 was associated to ECT2 in MDA-MB-231 cells to regulate Rac1 activity and therefore promote cell motility. Using *Xenopus laevis* embryos, we showed that Prickle1 and Ect2 acted synergistically during embryonic development. Together these data demonstrate the importance of Prickle1 and its associated protein complex as poor-prognosis markers in TNBC and give evidence that PRICKLE1 can be a suitable therapeutic target for treatment of still lacking targeted therapy for this aggressive subtype.

Results

Mass spectrometry analysis of the PRICKLE1 complex shows that PRICKLE1 is associated with small G-protein regulators and modulates Rac and Rho activity

We and others have shown that PRICKLE1 contribute to cancer cell dissemination in various cancers(Daulat et al 2016, Lim et al 2016, Luga et al 2012, Zhang et al 2016). To investigate the molecular mechanisms underlying the role of PRICKLE1 in tumorigenicity, and notably cell motility and dissemination, we generated a stable cell line expressing GFP-PRICKLE1 in the MDA-MB-231 highly invasive TNBC cell line. To identify protein complexes associated to PRICKLE1 in these cells, we performed anti-GFP immunoprecipitation followed by mass spectrometry analysis. We identified previously known PRICKLE1 interactors such as VANGL1, MINK1, RICTOR, LL5β, PLK1, and USP9x, validating our approach (**Fig. 1A**). Cell migration is a complex and dynamic process that involves continuous remodeling of the cellular architecture and relies on spatiotemporal modulation of signaling networks including Rho-family GTPases. Our attention was attracted by the large number of regulators of Rho-family GTPases such as Rac1, Rho and Cdc42 (**Fig. 1B**), known to be notably involved in the regulation of cell motility and considered as interesting drug targets to prevent cancer dissemination.

Prognosis value of PRICKLE1-interacting small G-protein regulators in TNBC

Based on our generated proteomic data describing the protein complex associated to PRICKLE1, we focused our attention on the 10 regulators of small G-proteins (i.e. Rho-GEF and Rho-GAP) identified, including ARHGAP21, ARGHAP22, ARHGAP23, ARHGEF2, ARHGEF40, BCR, ECT2, IQGAP3, MYO9B and STARD13. We assessed the mRNA expression level of the corresponding genes in a retrospective series of 8,982 clinically

annotated patients with invasive primary breast cancer gathered from several public data bases (**Table S1**). Within these 10 genes, *ECT2*, *IQGAP3* and *MYO9B* were the most overexpressed in tumors as compared to normal breast (**Fig. 2A**), whereas *ARHGEF40* and *STARD13* showed the lowest expression levels. We built a metagene including these 10 genes and compared its expression level in three molecular subtypes of breast cancer (RH+/HER2-, HER2+, and TN). The metagene was significantly up-regulated in the TN subtype comparatively to the two others subtypes ($p<1.0 \times 10^{-250}$, Anova) (**Fig. 2B**).

We then searched for correlations between the GAP-GEF metagene expression (as binary variable) and the clinicopathological features of samples, including MFS. Within the 8,982 breast cancer samples analyzed, 4,491 tumors (50%) showed metagene upregulation when compared with normal breast (ratio T/NB ≥ 2; ‘‘metagene-up’’ group), and 4.491 (50%) did not (ratio <2; ‘‘metagene-down’’ group) (**Table 1**). We found significant correlations between the metagene status and patients’ age ($p<0.001$), grade ($p<0.001$), ER ($p<0.001$), PR ($p<0.001$), and HER2 ($p=0.012$) statutes and as shown above with molecular subtypes. MFS data were available for 2,030 patients: the 5-year MFS was 75% (95 Cl, 72-79) in the “metagene-down” group *versus* 67% (95Cl, 63-71) in the “metagene-up” group ($p=0.00023$, log-rank test; **Fig. 2C**). In fact, such prognostic correlation was only observed in TNBC patients, and not in the non-TNBC ones ($p=0.461$, log rank test; **Fig. 2D**). In TNBC patients, the 5-year MFS was 77% (95 Cl, 66-90) in the “metagene-down” group *versus* 60% (95Cl, 54-66) in the “metagene-up” group ($p=0.029$, log-rank test; **Fig. 2E**).

Cooperation between PRICKLE1 and ECT2 as poor-prognosis marker in TNBC

We have previously shown that *PRICKLE1* upregulation is associated with poor MFS in basal breast cancer(Daulat et al 2016), a molecular subtype mainly composed of TNBC. In the present series of TNBC, we confirmed that *PRICKLE1* upregulation was associated with

151 shorter MFS, with 70% 5-year MFS (95Cl, 61-79) *versus* 55% (95Cl, 48-63) in the
152 *PRICKLE1*-down group and the *PRICKLE1*-up group respectively (p=0.0147, log-rank test)
153 (**Fig. 2F**). Since *PRICKLE1* and the 10 genes of the metagene interact together, we searched
154 for an eventual cooperation of their association in prognostic term. First, we analyzed the
155 combination of the metagene expression and *PRICKLE1* expression. Interestingly, patients
156 with upregulation of both markers displayed shorter 5-year MFS (53%, 95Cl, 46-62) than
157 patients without upregulation of both markers (72%, 95Cl 60-88; p=0.017, log-rank test),
158 whereas patients with intermediate status (up and no-up, and vice-versa) showed intermediate
159 5-year MFS not significantly different from the same patients (p=0.757, and p=0.495
160 respectively, log-rank test; **Fig. 2G**). This data suggest that metagene expression and
161 *PRICKLE1* expression might provide complementary prognostic value. Such
162 complementarity between the two prognostic variables was tested in the TN patients using the
163 likelihood ratio (LR) test. As shown in **Table 2A**, the metagene tended to add prognostic
164 information to that provided by *PRICKLE1* expression (LR-ΔX2=2.75, p=0.097).
165 Second, because ECT2 was one of the most prominent hit identified by mass spectrometry
166 analysis (**Fig. 1B**) and the gene most overexpressed in TNBCs among members of the
167 metagene (**Fig. 2A**), we investigated whether *ECT2* expression alone (without the nine other
168 genes of the metagene) would be sufficient to improve the prognostic value of *PRICKLE1*
169 expression in TNBC patients. As shown in **Figure 2H**, patients with *ECT2* upregulation
170 displayed shorter 5-year MFS (56%, 95Cl 50-64) than patients without upregulation (70%,
171 95Cl 60-81; p=0.0243, log-rank test). More interestingly, ECT2 expression status increased
172 the prognostic value of *PRICKLE1* expression when combined. Patients with upregulation of
173 both genes displayed 50% 5-year MFS (95Cl, 46-62) *versus* 67% for patients with
174 intermediate status (up and down, and vice-versa) *versus* 76% (95Cl, 64-90) for patients
175 without upregulation of both markers (p=0.0134, log-rank test; **Fig. 2I**). The model

comparison (**Table 2B)** showed that such *ECT2* prognostic information added to that of *PRICKLE1* expression was statistically significant (LR-ΔX2=4.74, p=0.029), indicating that *ECT2* expression improved the prognostic value of *PRICKLE1* expression in TNBC.

PRICKLE1 binds to ECT2 through it PET domain and modulates Rac1 activity

We then sought to investigate the molecular mechanisms potentially associated to this cooperation of PRICKLE1 and ECT2 expressions to confer poor prognosis. ECT2 is a Rho-GEF and acts in non-cancerous cells as regulator of cytokinesis by exchanging GDP to GTP on the small GTPases, RhoA, Rac1 and Cdc42(Basant and Glotzer 2018). ECT2 is upregulated in human cancers and acts as oncogene(Jin et al 2014). In lung and ovarian cancer, ECT2 has a distinct role than cytokinesis and acts in the nucleus by recruiting Rac1 and effectors which are required for tumour initiation and transformation(Justilien and Fields 2009, Justilien et al 2011, Justilien et al 2017). ECT2 knockdown inhibits Rac1 activity leading to a decrease of tumorigenicity and invasion in lung adenocarcinoma(Justilien and Fields 2009). Recently, ECT2 has been described to be upregulated in breast cancer(Wang et al 2018). At the cellular level, ECT2 is localized in the cytoplasm of cancerous cells(Justilien et al 2011). To confirm our mass spectrometry analysis, we immunoprecipitated GFP-PRICKLE1 stably expressed in MDA-MB-231 cells using GFP-targeted antibody and we assessed the presence of ECT2 associated to PRICKLE1 immunoprecipitate by western blot analysis complex (**Fig. 3A**). We confirmed that ECT2 is associated with PRICKLE1 in MDA-MB-231 cells. We further confirmed that ECT2 colocalizes in actin-enriched structures of lamellipodia along with PRICKLE1 using MDA-MB-231 stably expressing GFP-PRICKLE1 (**Fig. 3B**). We next decided to map the domain of interaction between PRICKLE1 and ECT2. We thus generated deleted versions of PRICKLE1 lacking the PET and/or the LIM domains and a construct encompassing the PRICKLE1 C-terminal region. We co-transfected

HEK293T cells with the indicated flag tagged PRICKLE1 mutants with Cherry-ECT2. After Flag immunoprecipitation, we assessed the presence of Cherry-ECT2 by western blot analysis. We observed that the PET domain of PRICKLE1 was required for the formation of the PRICKLE1-ECT2 protein complex (**Fig. 3C**).

We further assessed PRICKLE1 contribution on Rac activity. We used previously characterized siRNAs(Daulat et al 2016) to specifically downregulate PRICKLE1 expression in MDA-MB-231 cells. We observed that PRICKLE1 modulated Rac1 activity, suggesting a prominent role of PRICKLE1 in the regulation of Rho-GEF and Rho-GAP (**Fig. 3D**). We next set up an essay to monitor the role of PRICKLE1 on ECT2 Rho GEF activity. We expressed cherry-ECT2 in HEK293T cells and observed an increase of active Rac1 (lane 2). However, when flag-PRICKLE1 was co-expressed with cherry-ECT2, we observed an inhibitory effect of PRICKLE1 (lane 3). This observation was confirmed by the co-expression of PRICKLE1 delta PET delta LIM1 which is unable to bind ECT2 and does not affect the gain of activity of ECT2 in our system (lane 4) (**Fig. 3E**). Altogether, our data suggest that PRICKLE1 is associated with ECT2 in actin-rich structures within the lamellipodia of the cells in order to modulate the activity of the ECT2 on Rac1.

Prickle1 and Ect2 functionally interact in Xenopus during embryonic development

PRICKLE1 is an evolutionary conserved protein and plays a pivotal role during gastrulation to modulate convergent-extension movements (CE), which are crucial to shape the body plan(Takeuchi et al 2003, Wallingford et al 2002a). To test whether Ect2 is required for the previously characterized function of Prickle1 during CE, we first compared and analyzed the RNA-seq profile of *prickle1* and *ect2* reported on the public XenBase repository(Session et al 2016) (data not shown). We noticed a sharp peak of zygotic *ect2* expression at stage 9, which decreases abruptly at stage 10, just before gastrulation and CE movements take place.

Zygotic *prickle1* expression also begins to increase at stage 9, reaching a maximum at stage 12 (mid gastrula), and gradually decreasing until the end of neurulation. We next performed *in situ* hybridization and detected expression of *ect2* RNA in the animal hemisphere up until stage 9 (**Fig. 4A**). Thus, *ect2* transcription appears to terminate when *prickle1* transcription starts. However, inspection of genome-wide proteomic data(Peshkin et al 2015) indicated that Ect2 protein levels were maintained during gastrulation, suggesting that Ect2 could cooperate with Prickle1 to regulate morphogenetic movements. To test this hypothesis, we performed Prickle1 and Ect2 knockdown through antisense morpholinos (MO) injections, and assessed CE problems (**Fig. 4B**). Injection of 40ng MO Prickle1 led to CE defects in 73% of embryos, in comparison to non-injected embryos (98%) or embryos injected with RFP as control (83%). This data is consistent with previously published results(Daulat et al 2012, Takeuchi et al 2003). We then injected 20ng of MO targeting Ect2 and we observed CE problems at a rate of 71%, phenocopying the effect observed with MO Prickle1 with narrower and shorter embryos at tailbud stage 28. We then defined subthreshold doses of individual Mo-Prickle1 (</=10ng) and Mo-Ect2 (</=10ng) that yielded moderate CE defects in this assay when injected separately into two blastomeres at 2-cell stage (18% and 12% CE defects, respectively). In contrast, co-injecting both MOs at subthreshold doses caused strong disruption of CE movements (67%), suggesting that Prickle1 and Ect2 functionally interact during *Xenopus* embryonic development.

Discussion

We and others have demonstrated the prominent role of PRICKLE1 during cancer progression(Daulat et al 2016, Lim et al 2016, Luga et al 2012, Zhang et al 2016). In this study, we identified the protein complex associated to PRICKLE1 and we aimed to evaluate the impact of PRICKLE1 and its associated protein complex in TNBC. Our results show that

PRICKLE1 acts as a scaffold protein due to the large number of associated proteins with enzymatic activity. Among the PRICKLE1-associated proteins, we focused our attention on small G-protein regulators since their impact on cell motility and cancer cell dissemination has been well characterized(Abreu-Blanco et al 2014, Cook et al 2014, Machacek et al 2009). Exploiting our transcriptomic breast cancer database, we showed that this subset of genes is up-regulated in TNBC. Among this group of genes, we identified *ECT2* as the most prominent contributor to *PRICKLE1* prognostic value. Indeed TNBC patient with up-regulated expression of both *PRICKLE1* and *ECT2* expression have a shorter MFS than other patients. We further characterized PRICKLE1 and ECT2 interaction and showed that PRICKLE1 controlled ECT2 function on Rac1 activation. We finally defined that Prickle1 and Ect2 interaction was evolutionary conserved, since both proteins contribute to *Xenopus* embryonic development and are involved in convergent-extension movements.

Among breast cancers, TNBC are considered as the most aggressive form and no targeted therapy is currently available due to a lack of specific targets(Tong et al 2018). Here, we show that *PRICKLE1* is overexpressed in TNBC and is a poor-prognosis marker. PRICKLE1 is a protein highly regulated by post-translational modifications, particularly through ubiquitination/deubiquitination. PRICKLE1 is indeed the target of SMURF1, an ubiquitin ligase, which allows its rapid degradation(Narimatsu et al 2009). PRICKLE1 is also protected from degradation by USP9x which de-ubiquitinates the protein(Paemka et al 2015). Interestingly USP9x is also up-regulated in several cancers and is considered as a poor-prognosis marker(Murtaza et al 2015). PRICKLE1 is also regulated through phosphorylation by the serine/threonine kinase called MINK1, which promotes its function, its membrane localization and association with signaling molecules(Daulat et al 2012). Together, this shows that PRICKLE1 is a pivotal protein in cancer cell dissemination and a candidate for setting up novel therapeutic strategies.

During developmental processes and cancer progression, PRICKLE1 is required for oriented cell migration(Chiapparo et al 2016, Daulat et al 2016, Lim et al 2016, Luga et al 2012). At the molecular level, we and others have shown that PRICKLE1 contributes to localize VANGL at the plasma membrane(Daulat et al 2012, Jenny et al 2003), LL5β at the +ends of the microtubules(Lim et al 2016), and to restrict localization of the Rho-GAP at the edge of the migrating cancer cells(Zhang et al 2016). PRICKLE1 also regulates spatial localization of several active proteins such as mTORC2 to allow local activation of Akt at the leading edge of migrating cells(Daulat et al 2016), PHLDB2 to disassemble focal adhesions(Lim et al 2016) and to restrict RhoA activity by regulating subcellular localization of Rho-GAP(Zhang et al 2016). Together the contribution of PRICKLE1 to localization of its interacting partners allows the cells to coordinate cellular movements to create a cellular imbalance and promote directed cell migration. Here we showed that PRICKLE1 also contribute to regulate the activity of ECT2, a GEF for Rac1, which is essential for cell motility.

ECT2 is a Rho-GEF controlling Rac1 activity(Justilien and Fields 2009). Although ECT2 has been extensively studied for its role in the nucleus and during cytokinesis, reports have shown that ECT2 can also be localized in the cytoplasm of cancerous cells(Justilien et al 2011). We observed that ECT2 is localized in actin-rich structures within the lamellipodia. As described for other PRICKLE1 interactors, PRICKLE1 might contribute to ECT2 spatial localization in order to modulate its Rac activity. Moreover, our data show that overexpression of ECT2 in HEK293T cells contributes to an increase of Rac activity, and that PRICKLE1 overexpression leads to a decrease of this gain of function, suggesting an inhibitory role of PRICKLE1 on ECT2 activity. Altogether, this depicts PRICKLE1 as a master regulator of localized expression and regulation of signaling events in migratory cancer cells.

Our data also identified a role for the PET domain of PRICKLE1, as ECT2 is to date the only protein identified to be associated with this domain. At the molecular level, it has been shown that PRICKLE1 exists in an open and closed conformation(Sweede et al 2008). It has been suggested that in closed conformation, the three LIM domains of PRICKLE1 mask the PRICKLE1 PET domain. In open conformation, the PET domain is unmasked, thus activating PRICKLE1. We can speculate that the interaction between PRICKLE1 and ECT2 can be modulated by switching between these two conformations providing a still uncharacterized molecular mechanism of PRICKLE1 activation.

Finally, our study identified that ECT2 acts during *Xenopus* embryonic development. Prickle1 has been extensively characterized for its contribution during convergent-extension(Takeuchi et al 2003, Veeman et al 2003) movements and has been shown to be asymmetrically distributed within cells in order to organize their movement(Ciruna et al 2006, Yin et al 2008). A previous study indicated that *Prickle1* mRNA accumulates within the blastopore lip from the onset of gastrulation(Wallingford et al 2002b). Here, we showed that *ect2* mRNA and presumably Ect2 protein are expressed prior to and in a broader pattern than Prickle1(Wallingford et al 2002b). Knockdown experiments strongly suggest that Prickle1 and Ect2 act together to allow convergence-extension movements during gastrulation. Altogether, our data support the view that Ect2 might represent a permissive factor for Prickle1 activity. This study demonstrates the importance of the evolutionary conserved interaction between Prickle1 and Ect2, which appears to be reactivated during tumorigenesis to promote cancer cell dissemination and metastasis.

Materials and Methods

Rac1 activity assay

Cells were lysed with ice cold lysis buffer (50 mM Tris, pH7.6, 150mM NaCl, 0.1% Triton X-100, 20mM $MgCl_2$ supplemented with protease inhibitor (Sigma)). Supernatant were collected after 10 min of centrifucation at 10,000xg at 4°C. Protein concentration is measured from the solubilized fraction and adjusted to 2mg/mL. 10% of the lysates are conserved as loading controls. 100µg of GST-CRIB are added to 2mg of lysate and incubate with rotation during 30 min at 4°C. Beads are then washed with 10 volumes of lysis buffer. Rac-GTP forms are eluted from the beads using 2x Leammli buffer. 30% of the sample are run on 15%SDS-PAGE gel and transfer to PVDF and blot with the indicated antibody.

Breast cancer samples and gene expression profiling

Our institutional series included 353 tumor samples from pre-treatment invasive primary mammary carcinomas either surgically removed or biopsied.(Sabatier et al 2011) The study was approved by our institutional review board. Each patient had given a written informed consent for research use. Samples had been profiled using Affymetrix U133 Plus 2.0 human microarrays (Santa Clara, CA, USA). We pooled them with 35 public breast cancer data sets comprising both gene expression profiles generated using DNA microarrays and RNA-Seq and clinicopathological annotations. These sets were collected from the National Center for Biotechnology Information (NCBI)/Genbank GEO, ArrayExpress, European Genome-Phenome Archive, The Cancer Genome Atlas portal (TCGA) databases, and authors' website (**Supplementary Table 1**). The final pooled data set included 8982 non-redundant non-metastatic, non-inflammatory, primary, invasive breast cancers.

Gene expression data analysis

Before analysis, several steps of data processing were applied. The first step was the normalization of each set separately. It was done in R using Bioconductor and associated

packages; we used quantile normalization for the available processed data from non-Affymetrix-based sets (Agilent, SweGene, and Illumina), and Robust Multichip Average (RMA) with the non-parametric quantile algorithm for the raw data from the Affymetrix-based sets. In the second step, we mapped the hybridization probes across the different technological platforms represented as previously reported.(Bertucci et al 2014) When multiple probes mapped to the same GeneID, we retained the most variant probe in a particular dataset. We log2-transformed the available TCGA RNA-Seq data that were already normalized. In order to avoid biases related to trans-institutional IHC analyses and thanks to the bimodal distribution of respective mRNA expression levels, the ER, progesterone receptor (PR), and HER2 statutes (negative/positive) were defined on transcriptional data of *ESR1,* *PGR,* and *HER2* respectively, as previously described.(Lehmann et al 2011) The molecular subtypes of tumors were defined as HR+/HER2- for ER-positive and/or PR-positive and HER2-negative tumors, HER2+ for HER2-positive tumors, and triple-negative (TN) for ER-negative, PR-negative and HER2-negative tumors. Next, expression levels of *PRICKLE1* and 10 genes of interest from the protein complex associated to Prickle1 (namely, *ARHGAP21*, *ARGHAP22*, *ARHGAP23*, *ARHGEF2*, *ARHGEF40*, *BCR*, *ECT2*, *IQGAP3*, *MYO9B,* and *STARD13*) were extracted from each of the 36 normalized data sets. Before analysis, gene expression levels were standardized within each data set using the PAM50 luminal A population as reference. This allowed to exclude biases due to laboratory-specific variations and to population heterogeneity and to make data comparable across all sets. *PRICKLE1* and *ECT2* upregulation in a tumor was defined by an expression level above median expression the other cases being defined as downregulation. GEF/GAP activity was based on metagene approach and computed on the mean of the 10 related genes standardized. GEF/GAP activity "up" was defined by a metagene score value above the global median of the metagene whereas other cases were defined as "down".

Statistical analysis

Correlations between tumor classes and clinicopathological variables were analyzed using the one-way analysis of variance (ANOVA) or the Fisher's exact test when appropriate. Metastasis-free survival (MFS) was calculated from the date of diagnosis until the date of distant relapse. Follow-up was measured from the date of diagnosis to the date of last news for event-free patients. Survivals were calculated using the Kaplan-Meier method and curves were compared with the log-rank test. The likelihood ratio (LR) tests were used to assess the prognostic information provided beyond that of PRICKLE1 model, GEF/GAP metagene or ECT2 model, assuming a χ^2 distribution. Changes in the LR values (LR-ΔX^2) measured quantitatively the relative amount of information of one model compared with another. All statistical tests were two-sided at the 5% level of significance. Statistical analysis was done using the survival package (version 2.30) in the R software (version 2.15.2; http://www.cran.r-project.org/). We followed the reporting REcommendations for tumor MARKer prognostic studies (REMARK criteria)(McShane et al 2005).

Xenopus embryo injections, plasmids, RNAs, and Mos

Eggs obtained from NASCO females were fertilized in vitro, dejellied and cultured as described previously(Marchal et al 2009). Wild-type embryos were obtained using standard methods(Franco et al 1999) from adult animals and staged according to Nieuwkoop and Faber (1994).

Ect2 riboprobe was generated from *Xenopus laevis* full-length Ect2 cDNA, obtained from Dharmacom™ (Plasmid XGC ect2 cDNA, Clone ID: 5083828; pCMV-SPORT6.ccdb). The cDNA was subcloned in pBS-SK vector. For *Ect2* sense probe the plasmid was linearized by

NotI and transcribed with T7 RNA polymerase. For *Ect2* antisense probe the plasmid was linearized by EcoRV and transcribed with T3 RNA polymerase.

Synthetic capped mRFP mRNA was produced using Ambion mMESSAGE mMACHINE Kit. pCS2-mRFP was linearized with NotI and mRNA was synthesized with Sp6 polymerase. 0,5ng of mRFP capped mRNA was used as injection control and tracer.

Morpholino antisense oligonucleotides (MO) were obtained from Genetools®, and the sequences were the following: Prickle1 (Pk1) 5'-CCTTCTGATCCATTTCCAAAGGCAT-3' (Dingwell and Smith 2006); ECT2 5'-TACTGGGAGAGCCATGTTTGATTT-3'. Embryos at 2-cell stage were injected in each blastomere with various doses of MOs. Embryos were cultured in modified Barth's solution until stage 28, when they were photographed.

Acknowledgements

The authors wish to thank Valérie Ferrier for critical review of the manuscript and Emilie Beaudelet for technical assistance with protein sample for mass spectrometry analysis. This work was funded by La Ligue Nationale Contre le Cancer (Label Ligue JPB and DB, and fellowship to AMD), Fondation de France (fellowship to AMD), Fondation ARC pour la Recherche sur le Cancer (grant to JPB and AS), INCA PLBIO INCa 9474 (fellowship to DR) and SIRIC (INCa-DGOS-Inserm 6038, fellowship to AMD). M.S.W. was a recipient of the Science without Borders PhD program from Brazil Coordenação de Aperfeiçoamento de Pessoal de Nível Superior (CAPES). The Marseille Proteomics (IBiSA) is supported by Institut Paoli-Calmettes (IPC) and Canceropôle PACA. Samples of human origin and associated data were obtained from the IPC/CRCM Tumor Bank that operates under authorization # AC-2013-1905 granted by the French Ministry of Research. Prior to scientific use of samples and data, patients were appropriately informed and asked to express their consent in writing, in compliance with French and European regulations. The project was

424 approved by the IPC Institutional Review Board. Jean-Paul Borg is a scholar of Institut
425 Universitaire de France.
426
427 **References**
428 Abreu-Blanco MT, Verboon JM, Parkhurst SM (2014). Coordination of Rho family GTPase
429 activities to orchestrate cytoskeleton responses during cell wound repair. *Curr Biol* **24:** 144-
430 155.
431
432 Basant A, Glotzer M (2018). Spatiotemporal Regulation of RhoA during Cytokinesis. *Curr*
433 *Biol* **28:** R570-R580.
434
435 Bertucci F, Finetti P, Viens P, Birnbaum D (2014). EndoPredict predicts for the response to
436 neoadjuvant chemotherapy in ER-positive, HER2-negative breast cancer. *Cancer letters* **355:**
437 70-75.
438
439 Butler MT, Wallingford JB (2017). Planar cell polarity in development and disease. *Nat Rev*
440 *Mol Cell Biol* **18:** 375-388.
441
442 Chiapparo G, Lin X, Lescroart F, Chabab S, Paulissen C, Pitisci L *et al* (2016). Mesp1
443 controls the speed, polarity, and directionality of cardiovascular progenitor migration. *J Cell*
444 *Biol* **213:** 463-477.
445
446 Ciruna B, Jenny A, Lee D, Mlodzik M, Schier AF (2006). Planar cell polarity signalling
447 couples cell division and morphogenesis during neurulation. *Nature* **439:** 220-224.
448

449 Cook DR, Rossman KL, Der CJ (2014). Rho guanine nucleotide exchange factors: regulators
450 of Rho GTPase activity in development and disease. *Oncogene* **33:** 4021-4035.
451
452 Daulat AM, Luu O, Sing A, Zhang L, Wrana JL, McNeill H *et al* (2012). Mink1 regulates
453 beta-catenin-independent Wnt signaling via Prickle phosphorylation. *Mol Cell Biol* **32:** 173-
454 185.
455
456 Daulat AM, Bertucci F, Audebert S, Serge A, Finetti P, Josselin E *et al* (2016). PRICKLE1
457 Contributes to Cancer Cell Dissemination through Its Interaction with mTORC2. *Dev Cell* **37:**
458 311-325.
459
460 Dingwell KS, Smith JC (2006). Tes regulates neural crest migration and axial elongation in
461 Xenopus. *Dev Biol* **293:** 252-267.
462
463 Franco PG, Paganelli AR, Lopez SL, Carrasco AE (1999). Functional association of retinoic
464 acid and hedgehog signaling in Xenopus primary neurogenesis. *Development* **126:** 4257-
465 4265.
466
467 Gubb D, Garcia-Bellido A (1982). A genetic analysis of the determination of cuticular
468 polarity during development in Drosophila melanogaster. *J Embryol Exp Morphol* **68:** 37-57.
469
470 Huff LP, Decristo MJ, Trembath D, Kuan PF, Yim M, Liu J *et al* (2013). The Role of Ect2
471 Nuclear RhoGEF Activity in Ovarian Cancer Cell Transformation. *Genes Cancer* **4:** 460-475.
472

Jenny A, Darken RS, Wilson PA, Mlodzik M (2003). Prickle and Strabismus form a functional complex to generate a correct axis during planar cell polarity signaling. *EMBO J* **22:** 4409-4420.

Jin Y, Yu Y, Shao Q, Ma Y, Zhang R, Yao H *et al* (2014). Up-regulation of ECT2 is associated with poor prognosis in gastric cancer patients. *Int J Clin Exp Pathol* **7:** 8724-8731.

Justilien V, Fields AP (2009). Ect2 links the PKCiota-Par6alpha complex to Rac1 activation and cellular transformation. *Oncogene* **28:** 3597-3607.

Justilien V, Jameison L, Der CJ, Rossman KL, Fields AP (2011). Oncogenic activity of Ect2 is regulated through protein kinase C iota-mediated phosphorylation. *J Biol Chem* **286:** 8149-8157.

Justilien V, Ali SA, Jamieson L, Yin N, Cox AD, Der CJ *et al* (2017). Ect2-Dependent rRNA Synthesis Is Required for KRAS-TRP53-Driven Lung Adenocarcinoma. *Cancer Cell* **31:** 256-269.

Lehmann BD, Bauer JA, Chen X, Sanders ME, Chakravarthy AB, Shyr Y *et al* (2011). Identification of human triple-negative breast cancer subtypes and preclinical models for selection of targeted therapies. *J Clin Invest* **121:** 2750-2767.

Lim BC, Matsumoto S, Yamamoto H, Mizuno H, Kikuta J, Ishii M *et al* (2016). Prickle1 promotes focal adhesion disassembly in cooperation with the CLASP-LL5beta complex in migrating cells. *J Cell Sci* **129:** 3115-3129.

Luga V, Zhang L, Viloria-Petit AM, Ogunjimi AA, Inanlou MR, Chiu E *et al* (2012). Exosomes mediate stromal mobilization of autocrine Wnt-PCP signaling in breast cancer cell migration. *Cell* **151:** 1542-1556.

Machacek M, Hodgson L, Welch C, Elliott H, Pertz O, Nalbant P *et al* (2009). Coordination of Rho GTPase activities during cell protrusion. *Nature* **461:** 99-103.

Marchal L, Luxardi G, Thome V, Kodjabachian L (2009). BMP inhibition initiates neural induction via FGF signaling and Zic genes. *Proc Natl Acad Sci U S A* **106:** 17437-17442.

McShane LM, Altman DG, Sauerbrei W, Taube SE, Gion M, Clark GM *et al* (2005). REporting recommendations for tumour MARKer prognostic studies (REMARK). *Br J Cancer* **93:** 387-391.

Murtaza M, Jolly LA, Gecz J, Wood SA (2015). La FAM fatale: USP9X in development and disease. *Cell Mol Life Sci* **72:** 2075-2089.

Narimatsu M, Bose R, Pye M, Zhang L, Miller B, Ching P *et al* (2009). Regulation of planar cell polarity by Smurf ubiquitin ligases. *Cell* **137:** 295-307.

Paemka L, Mahajan VB, Ehaideb SN, Skeie JM, Tan MC, Wu S *et al* (2015). Seizures are regulated by ubiquitin-specific peptidase 9 X-linked (USP9X), a de-ubiquitinase. *PLoS Genet* **11:** e1005022.

Peshkin L, Wuhr M, Pearl E, Haas W, Freeman RM, Jr., Gerhart JC *et al* (2015). On the Relationship of Protein and mRNA Dynamics in Vertebrate Embryonic Development. *Dev Cell* **35:** 383-394.

Sabatier R, Finetti P, Adelaide J, Guille A, Borg JP, Chaffanet M *et al* (2011). Down-regulation of ECRG4, a candidate tumor suppressor gene, in human breast cancer. *PLoS One* **6:** e27656.

Session AM, Uno Y, Kwon T, Chapman JA, Toyoda A, Takahashi S *et al* (2016). Genome evolution in the allotetraploid frog Xenopus laevis. *Nature* **538:** 336-343.

Sokol SY (2015). Spatial and temporal aspects of Wnt signaling and planar cell polarity during vertebrate embryonic development. *Semin Cell Dev Biol* **42:** 78-85.

Sweede M, Ankem G, Chutvirasakul B, Azurmendi HF, Chbeir S, Watkins J *et al* (2008). Structural and membrane binding properties of the prickle PET domain. *Biochemistry* **47:** 13524-13536.

Takeuchi M, Nakabayashi J, Sakaguchi T, Yamamoto TS, Takahashi H, Takeda H *et al* (2003). The prickle-related gene in vertebrates is essential for gastrulation cell movements. *Curr Biol* **13:** 674-679.

Tong CWS, Wu M, Cho WCS, To KKW (2018). Recent Advances in the Treatment of Breast Cancer. *Front Oncol* **8:** 227.

548 Veeman MT, Slusarski DC, Kaykas A, Louie SH, Moon RT (2003). Zebrafish prickle, a
549 modulator of noncanonical Wnt/Fz signaling, regulates gastrulation movements. *Curr Biol*
550 **13:** 680-685.
551
552 Wallingford JB, Fraser SE, Harland RM (2002a). Convergent extension: the molecular
553 control of polarized cell movement during embryonic development. *Dev Cell* **2:** 695-706.
554
555 Wallingford JB, Goto T, Keller R, Harland RM (2002b). Cloning and expression of Xenopus
556 Prickle, an orthologue of a Drosophila planar cell polarity gene. *Mech Dev* **116:** 183-186.
557
558 Wang HK, Liang JF, Zheng HX, Xiao H (2018). Expression and prognostic significance of
559 ECT2 in invasive breast cancer. *J Clin Pathol* **71:** 442-445.
560
561 Yin C, Kiskowski M, Pouille PA, Farge E, Solnica-Krezel L (2008). Cooperation of polarized
562 cell intercalations drives convergence and extension of presomitic mesoderm during zebrafish
563 gastrulation. *J Cell Biol* **180:** 221-232.
564
565 Zhang L, Luga V, Armitage SK, Musiol M, Won A, Yip CM *et al* (2016). A lateral signalling
566 pathway coordinates shape volatility during cell migration. *Nat Commun* **7:** 11714.
567
568 Zhou S, Wang P, Su X, Chen J, Chen H, Yang H *et al* (2017). High ECT2 expression is an
569 independent prognostic factor for poor overall survival and recurrence-free survival in non-
570 small cell lung adenocarcinoma. *PLoS One* **12:** e0187356.
571
572

Figure legends:

Figure 1: Mass spectrometry analysis of the PRICKLE1 protein complex from a TNBC cell line

A) Schematic representing the proteins associated to PRICKLE1 identified by mass spectrometry analysis from MDA-MB-231 cell extracts. Proteins have been classified following their function in several groups: Small G-proteins regulators, associated to cytoskeleton, Kinases, involved in Ubiquitination process, Membrane integrated, Scaffold proteins and others. B) Volcano plot showing the significance two-sample *t*-test (-Log p-value) *versus* fold-change (Log2 (GFP-PRICKLE1 versus GFP as control)) on the y and x axes, respectively. The full line is indicative of protein hits obtained at a permutation false discovery rate of 1% (pFDR). Data results from two different experiments processed three times. PRICKLE1 (the bait) is represented in red and ECT2 one of the most abundant PRICKLE1 associated partner is represented in green.

Figure 2: Prognosis value of PRICKLE1-interacting small G-protein regulators in TNBC and cooperation between *PRICKLE1* and *ECT2* as poor prognosis markers

A) Boxplot of GEF/GAP regulators expression across breast cancers. B) Boxplot of GEF/GAP regulators expression across triple negative (TN) *versus* HR+/HER2- or HER2+ breast cancer. C) Kaplan-Meier curves of metastasis-free survival among breast cancers patients according to overexpression (Up) *versus* underexpression (Down) of GEF/GAP metagene mRNA. D) Kaplan-Meier curves of metastasis-free survival among non-TNBC patients for GEF/GAP metagene mRNA expression. E) Kaplan-Meier curves of metastasis-free survival among TNBC patients for GEF/GAP metagene mRNA expression. F) Kaplan-Meier curves of metastasis-free survival among TNBC patients for *PRICKLE1* mRNA expression. G) Kaplan-Meier curves of metastasis-free survival among TNBC patients for

598 *PRICKLE1* mRNA and GEF/GAP metagene expression. H) Kaplan-Meier curves of
599 metastasis-free survival among TNBC patients for *ECT2* mRNA expression. I) Kaplan-Meier
600 curves of metastasis-free survival among TNBC patients for *PRICKLE1* and *ECT2* mRNA
601 expression.
602
603 **Figure 3: PRICKLE1 is associated to the Rho-GEF ECT2 and controls its activity**
604 A) Immunopurification of GFP-PRICKLE1 from MDA-MB-231 cell lysate using GFP
605 nanobodies coupled to sepharose beads allows the identification of ECT2 associated to
606 PRICKLE1. B) Immunofluorescence of MDA-MB-231 cells stably expressing GFP-
607 PRICKLE1 shows that ECT2 (endogenous) is colocalized with PRICKLE1 and enriched in
608 actin structures within the lamellipodia. C) Mapping of PRICKLE1 domain of interaction
609 with ECT2. HEK293T cells were co-transfected with the indicated form of PRICKLE1 (see
610 on the left for topology details) and Cherry-ECT2. After FLAG immunopurification, presence
611 of ECT2 is detected using anti-cherry antibody. D) Downregulation of PRICKLE1 expression
612 using siRNA targeting *PRICKLE1* shows an increase of Rac activity in MDA-MB-231 cells.
613 E) PRICKLE1 modulates ECT2 activity. Using HEK293T cells, we expressed or co-
614 expressed ECT2 with full length PRICKLE1 or a deleted version of PRICKLE1 lacking its
615 domain of interaction with ECT2. Overexpression of ECT2 leads to an increase of Rac
616 activity which was inhibited when PRICKLE1 is co-expressed. Co-expression of a mutant
617 form of PRICKLE1 did not modify the gain of function observed by ECT2 overexpression.
618
619 **Figure 4: Prickle1 and Ect2 functionally interact in Xenopus during embryonic**
620 **development**
621 A) *In situ* hybridization against *ect2* transcripts at stage 8, 9 and 10. *ect2* RNA is detectable in
622 the animal pole (animal view and lateral view) but not in the vegetal pole (vegetal view) at

623 stages 8 and 9, but no longer at stage 10. Schematic representations of embryos at the stages
624 analyzed are shown on the right. B) Embryos at 2-cell stage were injected into two
625 blastomeres with Prickle1 and Ect2 MOs as indicated. In all cases 0,5ng of *mRFP* mRNA was
626 injected as control and tracer. Suboptimal doses (10ng) of either MO did not cause CE
627 problems. However, when both Prickle1 and Ect2 MOs were co-injected at suboptimal doses
628 (5ng each), embryos displayed CE problems at a rate comparable to high doses of each MO
629 injected separately (40ng Prickle1-MO or 20ng Ect2-MO). A total of 60 embryos per
630 condition were analyzed in two independent experiments. Pictures illustrate representative
631 phenotypes. (SR=survival rate; ND=percentage of surviving embryos developing normally;
632 CED= percentage of surviving embryos showing convergent-extension defects). Scale bars: A
633 = 0,25 mm; B = 0,5mm.
634

FIGURE 1:

A

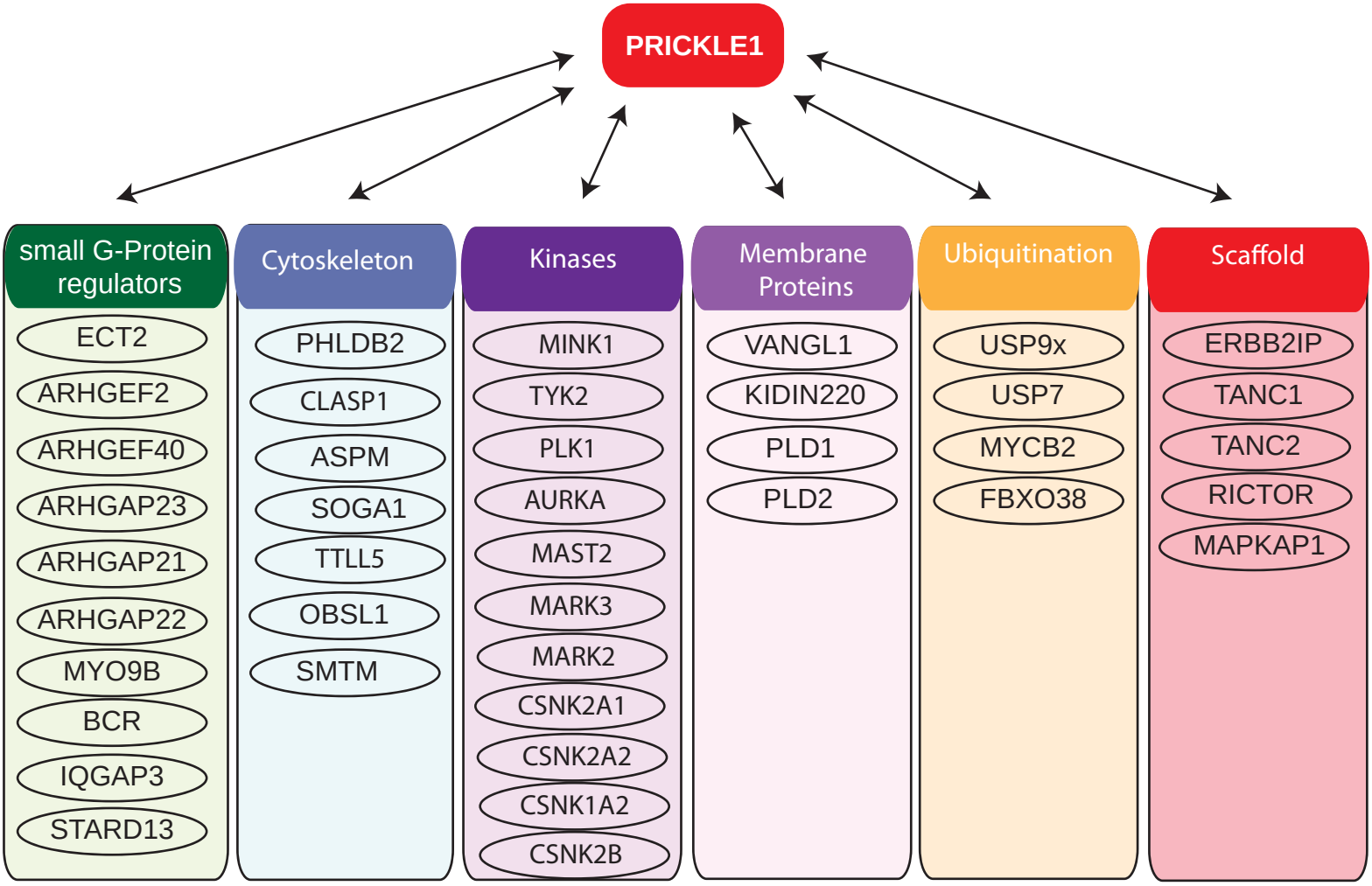
PRICKLE1
small G-Protein regulators
ECT2
ARHGEF2
ARHGEF40
ARHGAP23
ARHGAP21
ARHGAP22
MYO9B
BCR
IQGAP3
STARD13
Cytoskeleton
PHLDB2
CLASP1
ASPM
SOGA1
TTLL5
OBSL1
SMTM
Kinases
MINK1
TYK2
PLK1
AURKA
MAST2
MARK3
MARK2
CSNK2A1
CSNK2A2
CSNK1A2
CSNK2B
Membrane Proteins
VANGL1
KIDIN220
PLD1
PLD2
Ubiquitination
USP9x
USP7
MYCB2
FBXO38
Scaffold
ERBB2IP
TANC1
TANC2
RICTOR
MAPKAP1

B

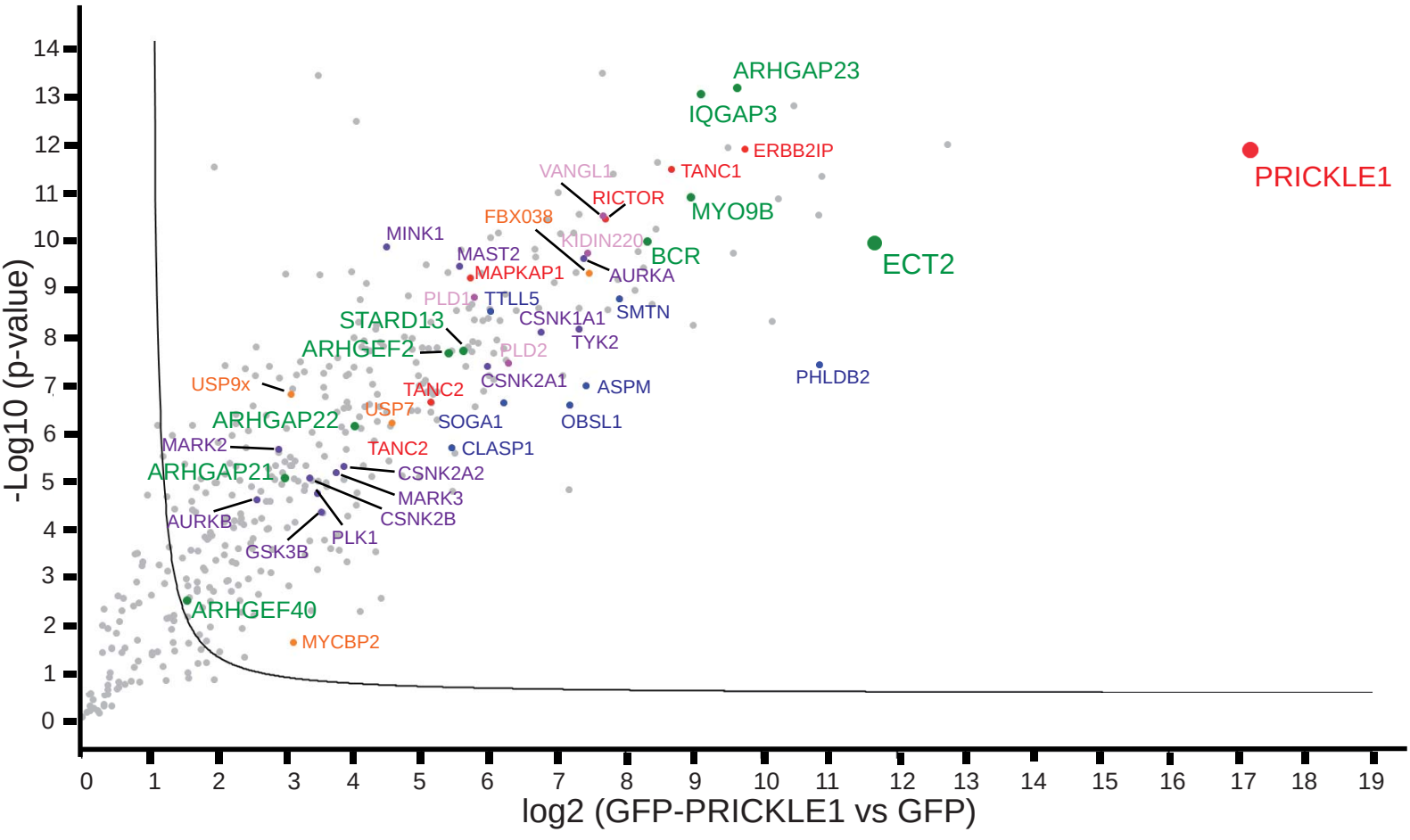
-Log10 (p-value)
log2 (GFP-PRICKLE1 vs GFP)
ARHGAP23
IQGAP3
ERBB2IP
PRICKLE1
VANGL1
TANC1
RICTOR
MYO9B
FBXO38
MINK1
KIDIN220
BCR
ECT2
MAST2
MAPKAP1
AURKA
PLD1
TTLL5
CSNK1A1
SMTN
STARD13
TYK2
ARHGEF2
PLD2
PHLDB2
USP9x
TANC2
CSNK2A1
ASPM
USP7
SOGA1
OBSL1
ARHGAP22
MARK2
TANC2
CLASP1
ARHGAP21
CSNK2A2
MARK3
AURKB
CSNK2B
PLK1
GSK3B
ARHGEF40
MYCBP2

FIGURE 2:

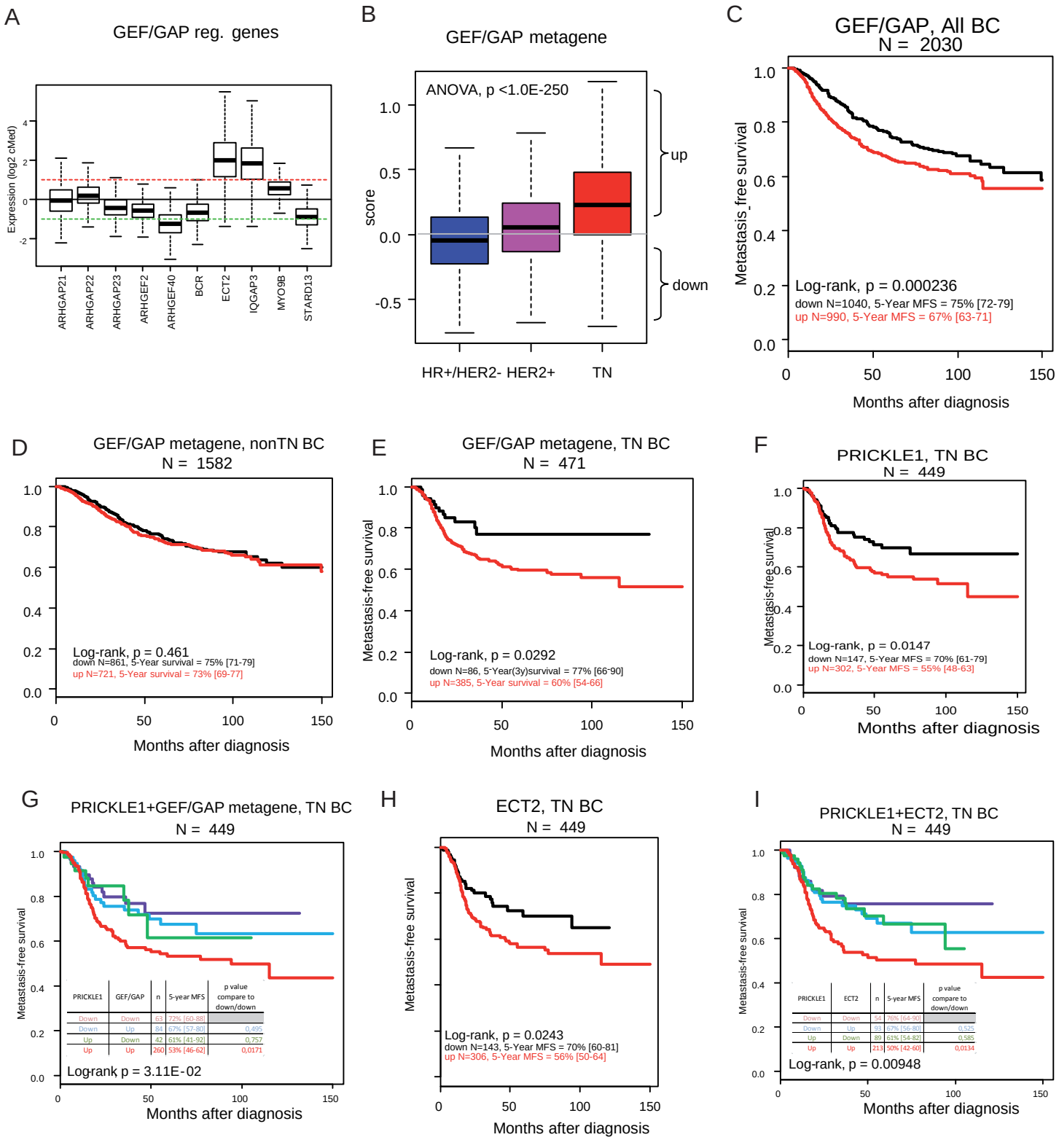
A
GEF/GAP reg. genes
Expression (log2 cMed)
ARHGAP21
ARHGAP22
ARHGAP23
ARHGEF2
ARHGEF40
BCR
ECT2
IQGAP3
MYO9B
STARD13
B
GEF/GAP metagene
ANOVA, p <1.0E-250
score
up
down
HR+/HER2-
HER2+
TN
C
GEF/GAP, All BC
N = 2030
Metastasis-free survival
Log-rank, p = 0.000236
down N=1040, 5-Year MFS = 75% [72-79]
up N=990, 5-Year MFS = 67% [63-71]
Months after diagnosis
D
GEF/GAP metagene, nonTN BC
N = 1582
Log-rank, p = 0.461
down N=861, 5-Year survival = 75% [71-79]
up N=721, 5-Year survival = 73% [69-77]
Months after diagnosis
E
GEF/GAP metagene, TN BC
N = 471
Metastasis-free survival
Log-rank, p = 0.0292
down N=86, 5-Year(3y)survival = 77% [66-90]
up N=385, 5-Year survival = 60% [54-66]
Months after diagnosis
F
PRICKLE1, TN BC
N = 449
Metastasis-free survival
Log-rank, p = 0.0147
down N=147, 5-Year MFS = 70% [61-79]
up N=302, 5-Year MFS = 55% [48-63]
Months after diagnosis
G
PRICKLE1+GEF/GAP metagene, TN BC
N = 449
Metastasis-free survival
PRICKLE1
GEF/GAP
n
5-year MFS
p value compare to down/down
Down Down 63 72% [60-88]
Down Up 84 67% [57-80] 0,492
Up Down 42 61% [41-92] 0,757
Up Up 260 53% [46-62] 0,0171
Log-rank p = 3.11E-02
Months after diagnosis
H
ECT2, TN BC
N = 449
Metastasis-free survival
Log-rank, p = 0.0243
down N=143, 5-Year MFS = 70% [60-81]
up N=306, 5-Year MFS = 56% [50-64]
Months after diagnosis
I
PRICKLE1+ECT2, TN BC
N = 449
Metastasis-free survival
PRICKLE1
ECT2
n
5-year MFS
p value compare to down/down
Down Down 54 76% [64-90]
Down Up 93 67% [56-80] 0,525
Up Down 89 61% [54-82] 0,585
Up Up 213 50% [42-60] 0,0134
Log-rank, p = 0.00948
Months after diagnosis

FIGURE 3:

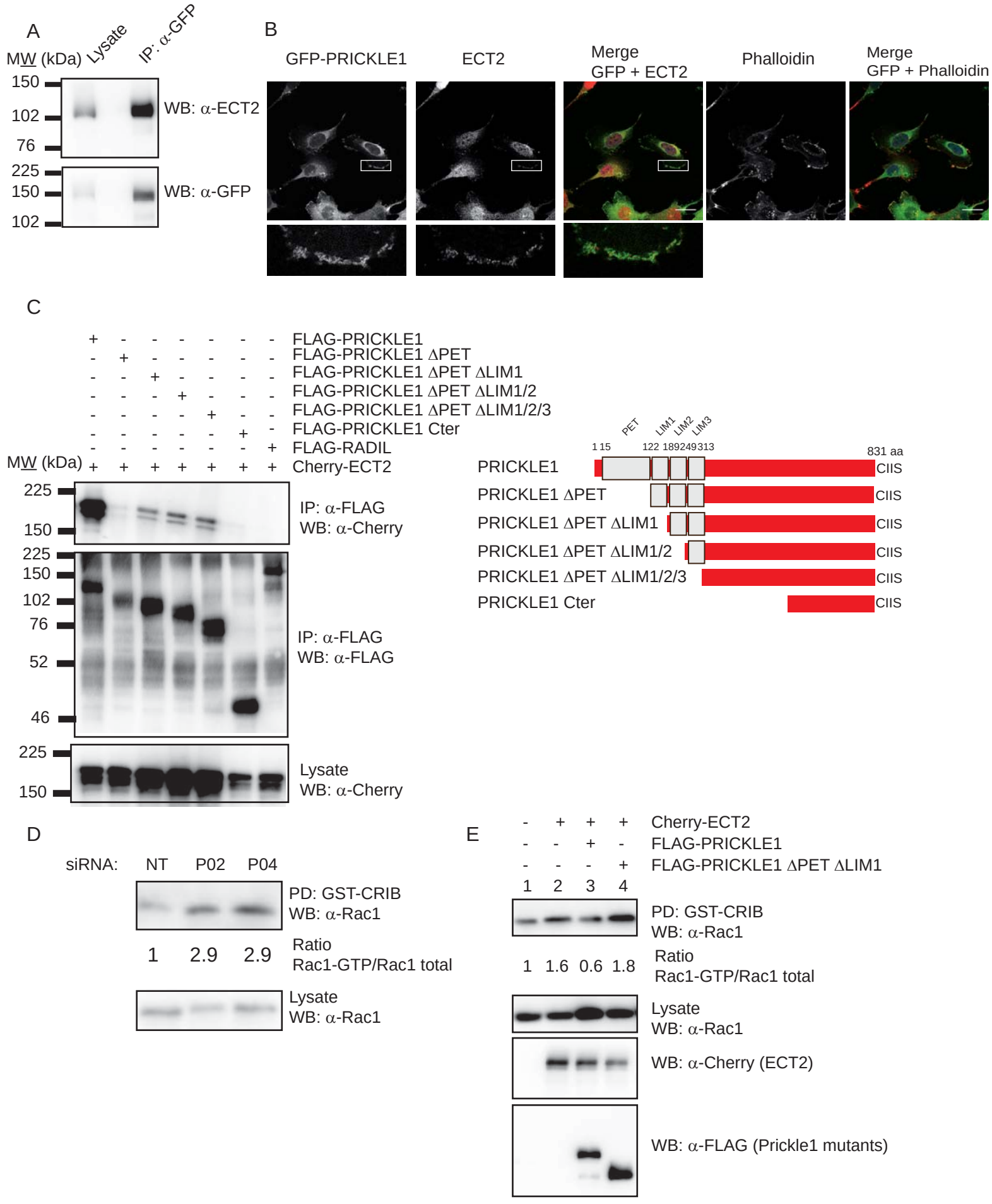
A
MW (kDa)
Lysate
IP: α-GFP
150
102
76
225
150
102
WB: α-ECT2
WB: α-GFP
B
GFP-PRICKLE1
ECT2
Merge GFP + ECT2
Phalloidin
Merge GFP + Phalloidin
C
FLAG-PRICKLE1
FLAG-PRICKLE1 ΔPET
FLAG-PRICKLE1 ΔPET ΔLIM1
FLAG-PRICKLE1 ΔPET ΔLIM1/2
FLAG-PRICKLE1 ΔPET ΔLIM1/2/3
FLAG-PRICKLE1 Cter
FLAG-RADIL
Cherry-ECT2
MW (kDa)
225
150
IP: α-FLAG
WB: α-Cherry
225
150
102
76
52
46
IP: α-FLAG
WB: α-FLAG
225
150
Lysate
WB: α-Cherry
PET
LIM1
LIM2
LIM3
1 15
122 189249313
831 aa
PRICKLE1
PRICKLE1 ΔPET
PRICKLE1 ΔPET ΔLIM1
PRICKLE1 ΔPET ΔLIM1/2
PRICKLE1 ΔPET ΔLIM1/2/3
PRICKLE1 Cter
CIIS
D
siRNA:
NT
P02
P04
PD: GST-CRIB
WB: α-Rac1
1
2.9
2.9
Ratio
Rac1-GTP/Rac1 total
Lysate
WB: α-Rac1
E
Cherry-ECT2
FLAG-PRICKLE1
FLAG-PRICKLE1 ΔPET ΔLIM1
1
2
3
4
PD: GST-CRIB
WB: α-Rac1
1
1.6
0.6
1.8
Ratio
Rac1-GTP/Rac1 total
Lysate
WB: α-Rac1
WB: α-Cherry (ECT2)
WB: α-FLAG (Prickle1 mutants)

FIGURE 4:

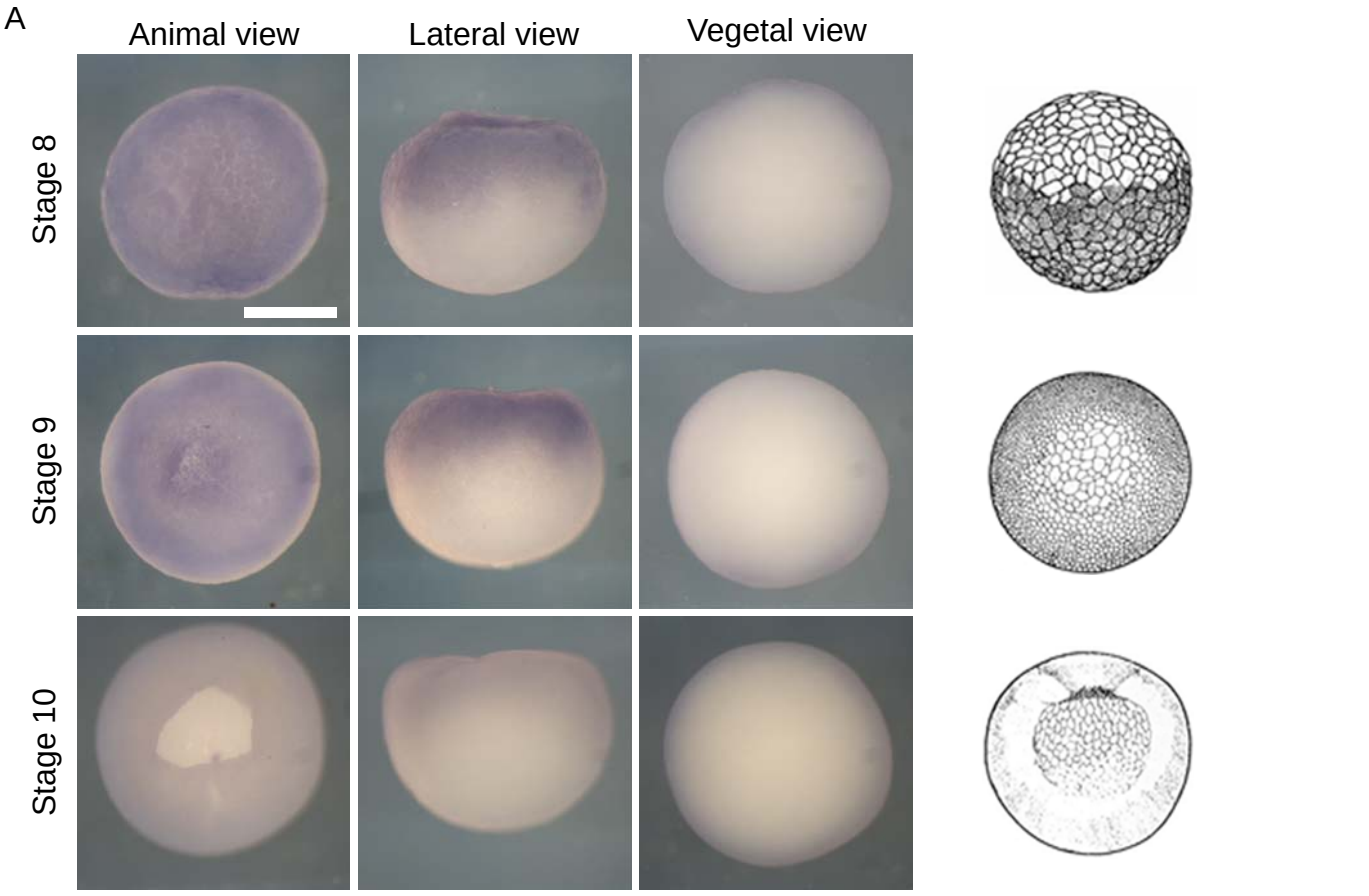

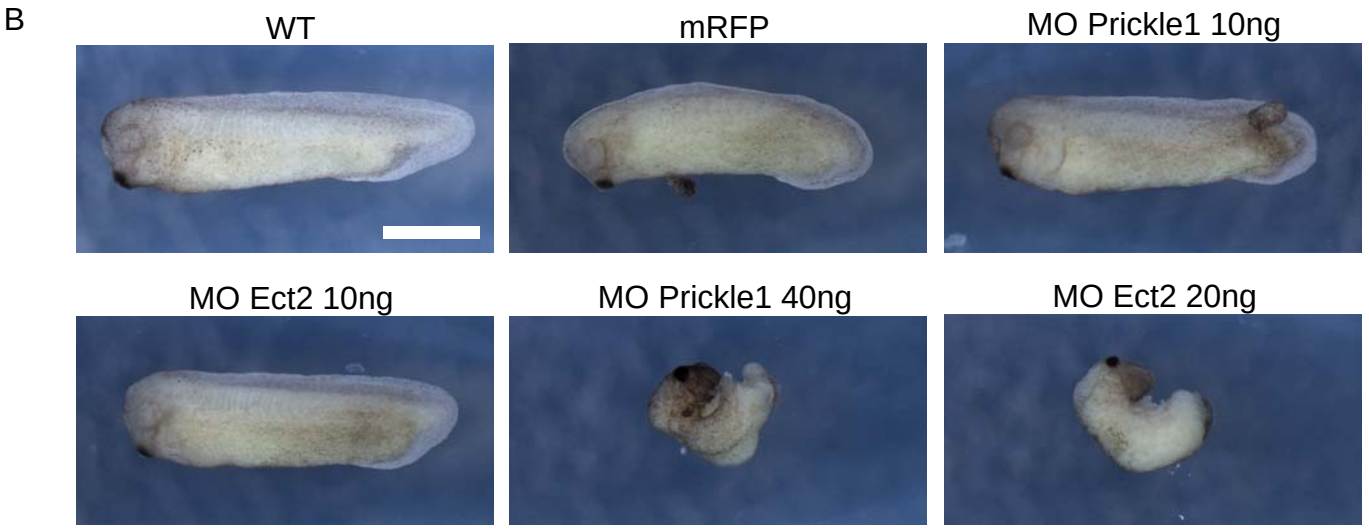

	SR %	ND %	DD %
WT	92	98	2
RFP	70	83	17
Mo Ect2 (10ng)	85	88	12
Mo Prickle1 (10ng)	82	82	18
Mo Ect2 (20ng)	63	29	71
Mo Prickle1 (40ng)	50	27	73
Mo Ect2 + Prickle1 (5ng+5ng)	45	33	67

Table 1:
Description GEF/GAP, all BC

Characteristics		N (%)	GEF/GAP down	GEF/GAP up	p-value
Age at diagnosis (years)					3,46E-14
	<=50	2540 (36%)	1112 (32%)	1428 (40%)	
	>50	4488 (64%)	2388 (68%)	2100 (60%)	
Pathological type					1,21E-02
	ductal	3979 (79%)	1998 (77%)	1981 (80%)	
	lobular	498 (10%)	263 (10%)	235 (10%)	
	other	574 (11%)	325 (13%)	249 (10%)	
Pathological tumor size (pT)					0,133
	pT1	2113 (38%)	1100 (39%)	1013 (36%)	
	pT2	2923 (52%)	1439 (51%)	1484 (53%)	
	pT3	595 (11%)	304 (11%)	291 (10%)	
Pathological axillary node status (pN)					0,239
	0	3446 (56%)	1741 (56%)	1705 (55%)	
	1	2743 (44%)	1344 (44%)	1399 (45%)	
Pathological grade					1,00E-06
	1	721 (11%)	442 (14%)	279 (9%)	
	2	2573 (41%)	1478 (48%)	1095 (34%)	
	3	2986 (48%)	1181 (38%)	1805 (57%)	
ER mRNA status					2,29E-153
	negative	2764 (31%)	811 (18%)	1953 (43%)	
	positive	6218 (69%)	3680 (82%)	2538 (57%)	
PR mRNA status					8,62E-53
	negative	4670 (52%)	1976 (44%)	2694 (60%)	
	positive	4255 (48%)	2489 (56%)	1766 (40%)	
ERBB2 mRNA status					0,00021
	negative	7884 (88%)	4000 (89%)	3884 (86%)	
	positive	1098 (12%)	491 (11%)	607 (14%)	
Molecular subtype					1,00E-06
	HR+/HER2-	5929 (66%)	3532 (79%)	2397 (54%)	
	HER2+	1098 (12%)	491 (11%)	607 (14%)	
	TN	1936 (22%)	463 (10%)	1473 (33%)	
Metastasis					6,81E-06
	no	3127 (77%)	1606 (80%)	1521 (74%)	
	yes	923 (23%)	396 (20%)	527 (26%)	
follow-up		42 (1-232	38 (1-221)	37 (1-232)	0,48
5-year MFS		71% [69-74]	75% [72-79]	67% [64-71]	5,09E-04

Table 2: Model of comparision

A, *PRICKLE1 & GEF/GAP*

MFS,TN BC	statistic		p-value
PRICKLE1	LRX^2	6,23	1,25E-02
PRICKLE1 + GEF/GAP	LRX^2	8,98	1,12E-02
GEF/GAP+PRICKLE1 vs. PRICKLE1	ΔLRX^2	2,75	0,097

B, *PRICKLE1 & ECT2*

MFS,TN BC	statistic		p-value
PRICKLE1	LRX^2	6,23	1,25E-02
PRICKLE1 + ECT2	LRX^2	11	4,14E-03
ECT2+PRICKLE1 vs. PRICKLE1	ΔLRX^2	4,74	2,90E-02